A KALMAN FILTER SINGLE POINT POSITIONING FOR MARITIME APPLICATIONS USING A SMARTPHONE

Anna INNAC [1,*], Antonio ANGRISANO [2], Gino DARDANELLI [3], Vincenzo DELLA CORTE [4], Elena MARTELLATO [1], Alessandra ROTUNDI [1], Giampaolo FERRAIOLI [1], Pasquale PALUMBO [1] and Salvatore GAGLIONE [1]

DOI: 10.21163/GT_2021.163.02

ABSTRACT

Different positioning techniques have been largely adopted for maritime applications that require high accuracy kinematic positioning. The main objective of the paper is the performance assessment of a Single Point Positioning algorithm (SPP), with a Kalman filter (KF) estimator, adapted for maritime applications. The KF has been chosen as estimation technique due to the ability to consider both the state vector dynamic and the measurements. Particularly, in order to compute an accurate vertical component of the position, suitable for maritime applications, the KF settings have been modified by tuning the covariance matrix of the process noise. The algorithm is developed in Matlab environment and tested using multi-GNSS single-frequency raw data, collected by a smartphone located on board a moving ship. The algorithm performance evaluation is carried out in position domain and the results show an enhancement of meter order on vertical component compared to the classical SPP based on Least Square estimation technique. In addition, different GNSSs configurations are considered to verify the benefits of their integration in terms of accuracy, solution availability and geometry.

Key-words: *Single Point Positioning; GNSS; Vessel; Smartphone*.

1. INTRODUCTION

The Global Navigation Satellite Systems (GNSS) is an essential instrument in maritime navigation, providing position, velocity and time (PVT) information. The main role of GNSS in applications like marine geodesy, offshore survey and physical oceanography is related to the ability of performing a highly precise kinematic positioning of surveying platforms such as buoys, vessels and aircrafts.

GNSS is adopted as main position system for dynamic positioning (DP) of vessels. The International Maritime Organization (IMO) and the certifying societies define a dynamically positioned vessel as a vessel that maintains its position and heading (fixed location or pre-determined track) only by means of active thrusters. Reference sensors, combined with motion sensors, gyrocompasses and wind sensors, provide information to the computer concerning the vessel's position and the amplitude and direction of environmental forces affecting its position (Sørensen, 2011).

[1]*Department of Sciences and Technologies, University of Naples Parthenope, Via Ammiraglio F. Acton, 80133 Naples, Italy; anna.innac@uniparthenope.it, salvatore.gaglione@uniparthenope.it, elena.martellato@uniparthenope.it, alessandra.rotundi@uniparthenope.it, giampaolo.ferraioli@uniparthenope.it, pasquale.palumbo@uniparthenope.it*

[2] *University of Benevento G. Fortunato, Via R. Delcogliano, 82100 Benevento, Italy a.angrisano@unifortunato.eu*

[3] *Department of Engineering, University of Palermo, Viale delle Scienze, 90128 Palermo, Italy; gino.dardanelli@unipa.it*

[4] *IAPS – INAF, Via del Fosso del Cavaliere,100, 00133 Rome, Italy; vincenzo.dellacorte@inaf.it*

Other GNSS maritime applications are related, for example, to the measures of sea level for validation/calibration of satellite radar altimetry. Information about the accurate positioning of ships and buoys, equipped with a GNSS, will contribute for the determining of the Sea Surface Height (SSH) to be used as a supplementary sensor for tsunami early warning system, combined to satellite altimetry data. GNSS measurements collected aboard a ship, for example, can be used as input parameter to algorithms computing the sea spectrum from the ship motion (IOC, 2006; Marreiros, 2013; Reinking & Härting, 2012; Alkan & Öcalan, 2013).

Different precise positioning techniques have been adopted for maritime applications, associated to accurate positioning requirements for maneuvering or anchoring floating platforms, DP vessel, sea level measurement and hydrographic surveying. GNSS precise positioning in the oceans is an attractive opportunity to be exploited. However, precise positioning of a moving ship is especially challenging due to the high dynamics of the antenna and the high reflectivity of the water (Alkan & Öcalan, 2013).

In this context, GNSS precise relative positioning techniques are widely adopted (Teunissen et al., 2011; Specht el al., 2019). The relative techniques are based on the use of a base receiver (or a network of base receivers), whose location is known, and exploit the concept of spatial correlation of several GNSS measurement errors. The classical differential GNSS technique using only pseudorange (PR) measurements provides meter level accuracy; decimeter or centimeter level accuracies can be obtained using carrier phase observable. To obtain the aforesaid performance, geodetic grade receivers and short baseline lengths are necessary. With short baseline lengths, a few kilometers, RTK (Real-Time Kinematic) is very accurate. However, as the baseline length increases, the accuracy and availability of a solution decreases. The constraint of the limited baseline lengths in RTK can be removed by using a method known as Network RTK (NRTK), whereby a network of reference stations with ranges usually less than 100 km is used (El-Mowafy, 2012). For these reasons, GNSS maritime applications are currently constrained to coastal areas and Precise Point Positioning (PPP) technique could be a valid alternative solution. In fact, PPP is increasingly becoming widespread as an absolute positioning technique since its capability to provide a precision level comparable to differential positioning through the use of a single GNSS receiver and appropriate correction models but without the support of ground stations. In addition, unlike the classical absolute positioning methods based on code measurements from four or more satellites and the broadcast ephemeris to obtain the position of the receiver, PPP has the advantage of using the most precise carrier phase observables, trying to reduce the effect of all the types of errors and biases that affect GNSS measurements.

Both RTK and PPP exploits the carrier-phase measurements, that are highly precise observations but very sensitive to signal obstruction and affected by an ambiguity which is unknown to the user and that can produce long converge time as necessary for PPP (Innac et al., 2018). The rapid development and use of combined multi-GNSS but also multi-frequency (triple and quadruple) observations may be beneficial for precise relative positioning performance. Number of new signal frequencies gives also opportunity for development of new ambiguity resolution algorithms that help to reduce the convergence time of the solution (Paziewski & Wielgosz, 2017). Furthermore, precise positioning is usually performed using high-quality, geodetic-grade GNSS receivers and antennas. These receivers are usually multi-frequency to mitigate the ionosphere influence and obtain faster ambiguity resolution, while the antennas are precisely calibrated to minimize the influence of the errors related to the antenna, and designed to reduce multipath effects. The cost of the previously mentioned equipment is very high, compared to mass-market receivers (Constantin-Octavian, 2012).

Because of technological advances, the potential of low-cost GNSS receivers and antennas has been investigated by scientific community. Low-cost GNSS hardware comprises chipsets, used also in smart devices. Indeed, the current smartphones are very advanced devices, equipped, among other things, with GNSS receivers, multi-axis accelerometers, gyroscopes and other sensors available for different applications.

Furthermore, recent smartphones receive signals from multiple GNSS systems, allowing to increase the satellite navigation performance as well-known by literature (Innac et al., 2018). In addition, the ability to access GNSS raw observables is an interesting feature since the developers are able to implement their own algorithm to compute positioning solution (Specht el al., 2019).

The opportunity of smart devices has been exploited by scientific community to carry out studies on signal quality, to develop algorithms aimed at enhancing the positioning accuracy of mass-market devices, and for several applications (Realini et al., 2017; Lachapelle et al., 2018; Robustelli et al. 2019; Paziewski, 2020).

The aim of the current work is to provide a low-cost alternative with lower performance to the common precise positioning techniques, obtained with RTK or PPP, implementing a Single Point Positioning (SPP) algorithm, with a Kalman filter (KF) estimator, able to achieve an accurate estimate of the position, especially for vertical component. The KF is a recursive algorithm based on a series of prediction and update phases to obtain an optimal state vector estimate (Angrisano et al., 2013). The KF includes a measurement model, formally identical to the one used in Least Square (LS) estimator, and a process model, representing the behavior of the state. Multi-GNSS single-frequency raw data collected by a smartphone are processed by the developed processing technique and different GNSSs combinations are considered, in order to verify the benefit of multi-GNSS integration in maritime context. The proposed algorithm can be suitable for maritime applications conducted on small boats not equipped with expensive sensors and it is especially performing in estimating the vertical component of the position, which is very useful for the analysis of the sea conditions (Montazeri et al., 2016; Piscopo et al., 2020). The positioning algorithm is tested on real data, collected by a smartphone Xiaomi Mi 8 located on board a moving ship; the receiver is a multi-GNSS, GPS, Glonass and BeiDou, device. To perform an error analysis, a ground truth trajectory is computed processing the collected dataset in differential mode.

The paper is organized as follow: section 2 describes the theoretical concepts of the developed algorithm, section 3 describes the test configuration and ground truth trajectory computation, section 4 provides a description of the experimental results and section 5 concludes the paper.

2. MULTI-GNSS SPP ALGORITHM

In this section, an overview of the adopted multi-GNSS SPP algorithm is provided. In detail, PR measurements from GPS, Glonass and BeiDou systems are processed and the KF estimation method is applied to compute position. The KF filter settings have been adapted for the considered application in order to obtain high accuracy on vertical component of the position. The EKF has the advantage to take in account, in addition to measurements information, also the dynamic model, whose uncertainty is expressed by covariance matrix of the process noise. In detail, the covariance matrix of the process noise has been configured using lower variance values for vertical component of the position in accordance with the behavior of the altitude of the moving vessel.

Even if GPS, Glonass and BeiDou are based the same operational principle, they have some differences related to signal, constellation and reference categories. These differences are largely detailed in literature (Li et al., 2015). When multi-GNSS observations are used to compute the navigation solution, the aforesaid differences are considered as detailed in (Angrisano et al., 2013). The theoretical concepts by the literature are applied in the current work as briefly described below. A customized PVT algorithm has been developed in MatLab® environment as detailed in (Angrisano et al., 2013) and belongs to a Toolbox developed by authors, who are members of PANG (PArthenope Navigation Group – http://pang.uniparthenope.it).

2.1. Multi-GNSS SPP

The standard PVT algorithm is based on PR observables, whose expression is:

$$PR = d + c\delta t_u - c\delta t_s + \Delta I + \Delta T + \varepsilon \quad (1)$$

where d is the range between the receiver and the satellite, δt_u and δt_s are the receiver and satellite clock offsets, c is the speed light, ΔT and ΔI are, respectively, the errors due to the tropospheric and ionospheric effects, and ε represents the residual errors. In detail, single-frequency raw PR measurements are corrected for the satellite clock error, using the parameters broadcast within GNSS navigation message. Furthermore, Saastamoinen and Klobuchar models are used, respectively, for the tropospheric and ionospheric delays correction (Hoffmann-Wellenhof et al., 1992; Kaplan, 2006; Angrisano et al., 2013).

Starting from nominal values of receiver clock offset and user position, indicated as $\underline{x}_0 = [x_0, y_0, z_0, c\delta t_0]^T$, the equation (1) must be linearized by a Taylor series expansion, truncated at the first order (Kaplan, 2006). The linearized measurement model describing the relationship between the state and the measurement at the current time step *k* is given by the following equation:

$$\underline{z}_k = H_k \cdot \underline{\Delta x}_k + \underline{\varepsilon}_k \tag{2}$$

In the above equation, the terms are defined as follows:
$\underline{z}_k$ is the measurements vector containing the differences between measured and computed PRs;
H_k is the geometry matrix;
$\underline{\varepsilon}_k$ is the measurement noise vector that is assumed to be zero-mean Gaussian with the covariance *R*, i.e., $\underline{\omega}_k \sim N(0, R)$;
$\underline{\Delta x}_k$ is the state vector of the linearized measurement model, containing the position and clock offsets from the linearization point.

Moreover, if multi-GNSS observations are used, the offset with respect to a time reference system, the inter-system offset, is considered for each new additional GNSS constellation.

Using an estimation method, the unknown components of the state vector $\underline{\Delta x}$ can be obtained. So, the user coordinates, the receiver clock and inter-system offsets can be obtained updating the approximate estimates as follows:

$$\underline{x}_k = \underline{x}_0 + \underline{\Delta x}_k \tag{3}$$

2.2. Extended Kalman Filter

To estimate the state vector, an Extended Kalman filter (EKF) estimator is used, that is the nonlinear type of the KF (Kalman, 1960) but able to provide the optimal solution to the linearized problem, fitting well with the considered application. In the current work, the EKF settings have been empirically tuned starting from reference values provided by literature (Kalman, 1960; Parkinson et al., 1996; Welch & Bishop, 2004). Furthermore, the measurements collected by the smartphone are characterized by higher noise than other types of receivers. In order to reduce the effects of the higher measure noise level, the covariance matrix of the process noise has been set using larger values of variance respect to the classical reference values.

The EKF estimation technique is based on knowledge about measurements and state vector dynamics adopting both measurement (2) and process models (4). The process model is given by following equation:

$$\underline{\Delta x}_{k+1} = \Phi_{k+1} \cdot \underline{\Delta x}_k + \underline{\omega}_k \tag{4}$$

where the transition matrix is indicated by Φ_{k+1} and $\underline{\omega}_k$ is the process noise vector, assumed zero-mean Gaussian with the covariance *Q*, i.e., $\underline{\omega}_k \sim N(0, Q)$.

KF is recursive, consisting of a series of prediction and update steps to obtain the optimal estimate of the state vector. Storing only the last filter computation result helps out in storage space issues effectively (Kalman, 1960; Parkinson et al., 1996; Welch & Bishop, 2004; Angrisano et al., 2013).

The first step of EKF is the prediction of the state vector, $\underline{\Delta x_k}$, and the associated covariance matrix, P_k , starting from the assumed process model:

$$\underline{\Delta x_k^-} = \Phi_k \cdot \underline{\Delta x_{k-1}^+} \tag{5}$$

$$P_k^- = \Phi_k P_{k-1}^+ \Phi_k^T + Q_k \tag{6}$$

In the above expressions the superscript "-" indicates a predicted quantity (i.e. before updating the measurements) and the superscript "+" refers to the corrected quantity (i.e. after the update of the measurements). The term Q_k is the covariance matrix of the process noise and indicates uncertainty in dynamic models.

In this work, the covariance matrix of the process noise is fine-tuned in order to obtain a more accurate estimation of vertical component of position, assigning suitable values to the components of the position. In particular, lower variance values are set for Q_k element corresponding to vertical component.

After the prediction step, the update phase is used to correct the state vector and the associated covariance matrix according to the measurement model. The EKF correction equations are:

$$\underline{\Delta x_k^+} = \mathrm{K}_k \cdot (\underline{z_k} - H_k \widehat{\underline{\Delta x_k^-}}) \tag{7}$$

$$P_k^- = \Phi_k P_{k-1}^+ \Phi_k^T + Q_k \tag{8}$$

The Kalman gain matrix K_k is defined as

$$\mathrm{K}_k = P_k^- H_k^T (H_k \, P_k^- H_k^T + R_k)^{-1} \tag{9}$$

where R_k is the measurements error covariance matrix and, in the current research, is defined as function of satellite elevation as in (Angrisano et al., 2013) for all GNSSs .

The Kalman gain matrix is a weighting factor that is multiplied to the difference between the actual measurement vector $\underline{z_k}$ and the predicted measurement vector $H_k \underline{\Delta x_k^-}$ This term is referred to as innovation vector and describes the amount of information introduced by the current measurements in the system. Consequently, the Kalman gain matrix indicates how much the final state vector estimate is influenced by the new information contained in the innovation vector (Angrisano et al., 2013).

The process model must be selected according to the user dynamics, in order to obtain satisfying performance; the position states are usually modeled as random walk or Gauss-Markov processes (P model) for a stationary user located at an unknown location. Instead, velocity or acceleration states are modeled as random walk processes (PV or PVA models), respectively, for user with low or high dynamics as described in (Welch & Bishop, 2004). In the current work, PV model is used as process model to obtain the best position estimates using data collected in kinematic mode as described in sub-section 3.1.

In **Fig. 1**, an overview of the developed SPP algorithm is provided. The main inputs of the algorithm are GNSS pseudorange observables and ephemerides. The ephemerides are used to compute satellite position and clock offset; different orbital propagators are implemented for the various GNSSs considered due to the different parameterization of the ephemerides.

The raw PR measurements are corrected as described in section 2.1 and used in the EKF or Weighted Least Square (WLS) estimator techniques to estimate epoch-by-epoch the positioning solution. Finally, the error analysis is carried out in position domain comparing the computed solution to the reference.

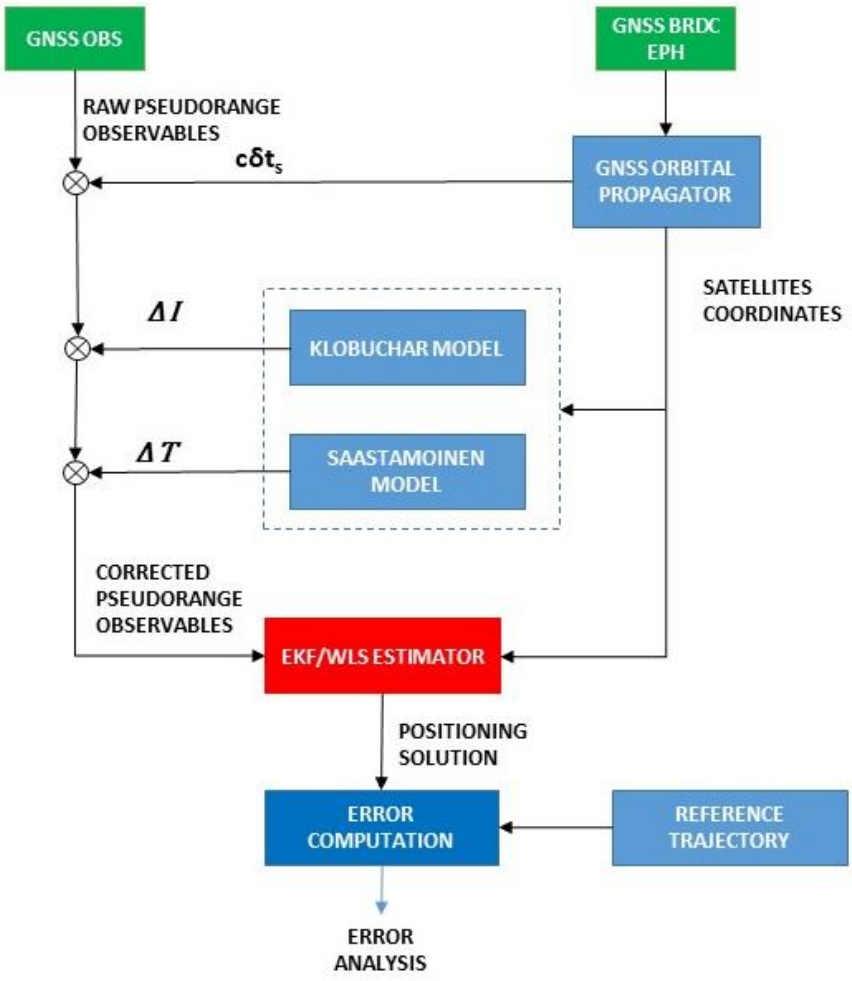

Fig. 1. SPP algorithm

3. TESTS

In this section a description of experimental setup is provided, detailing the configuration of the kinematic test in sub paragraph 3.1. To evaluate the performance of the proposed algorithm, error analysis in the position domain is carried out. Since for a kinematic test the computation of the reference trajectory is a challenging problem, in this study the data collected has been processed in differential mode, using data from a reference station as described in sub-paragraph 3.2.

3.1. Kinematic data collection

The performance of the proposed multi-GNSS SPP algorithm are evaluated processing real data in kinematic mode using a smartphone located onboard a ferry-boat travelling Mediterranean Sea on 18th of august 2019. Start and end points locations of the test are shown in **Fig. 2** and travelled distance is about 29 km.

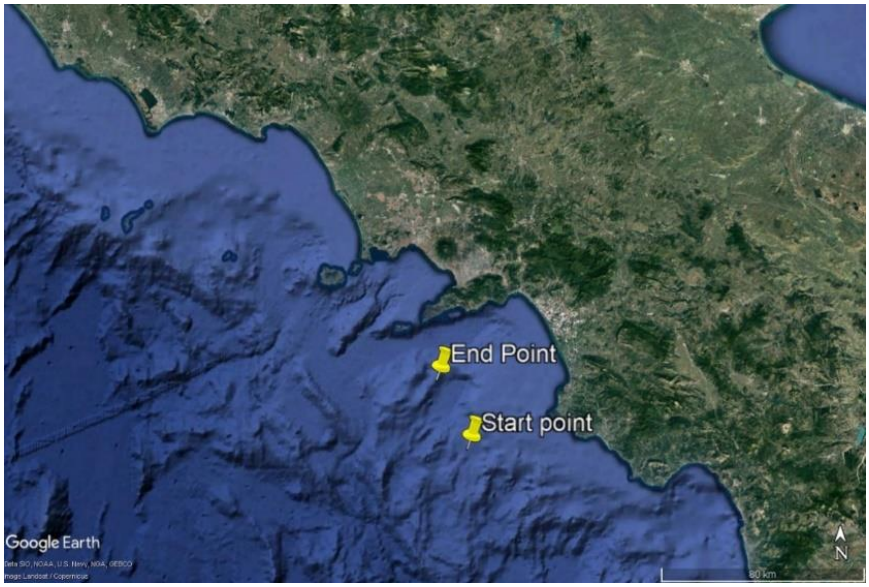

Fig. 2. Start and end points of the kinematic test performed using a smartphone onboard a ferry-boat on 18th of august 2019 (image acquired from Google Earth V. 7.3.3.7786)

One hour of 1 Hz measurements, collected on GPS L1, Glonass G1 and BeiDou B1 signals, are collected using Xiaomi Mi 8 located approximately in the centre of mass of the boat and Rinex ON application is used to store the raw observables in a RINEX (Receiver Independent Exchange Format) file. The Xiaomi Mi 8 is an Android smartphone equipped with a Broadcom BCM47755 chipset that is a dual-frequency GNSS chip able to track navigation messages, PR observables, accumulated delta ranges for GPS, Glonass, BeiDou and Galileo. However, during the considered test no Galileo satellites were tracked, probably due to a failure of the receiver or the logging application.

3.2. Reference trajectory

To perform an error analysis in position domain, a reference trajectory is obtained processing the kinematic dataset collected by the Xiaomi in differential mode using data from a permanent station located in Sorrento (SORR, Naples) and belonging to Leica ItalPoS network. Only code measurements have been used since the collected carrier phase measurements were noisy and un-continuous. It is well-known that smartphone GNSS observations are affected not only by measurement noise and multipath but also by anomalies such as gradual accumulation of phase errors and duty cycling. These phenomena limit the use of smartphone phase measurement to high-precision techniques such as RTK or PPP as described in (Paziewski et al., 2019). The analysis of smartphone signal quality confirmed the divergence between code and phase observations and poor quality of the latter.

In the present work, two different software have been used to compute the reference solution and both tools have not been able to effectively use carrier-phase measurements.

The two software used to compute the ground truth in this research, are:

- RTKlib ver. 2.4.3 b33, an open source positioning software developed by Dr. T.Takatsu (Takasu et al., 2007). Using the software Graphic User Interface, all the data and corrections are inserted as inputs. It supports standard and precise positioning algorithms with multi-GNSS (GPS, Glonass, Galileo, QZSS, BeiDou and SBAS) observations. For the aim of the paper, "DGPS/GNSS" (Code-based differential) has been chosen as positioning mode, using dual-frequency observations from GPS, Glonass and BeiDou systems. In addition, the

broadcast ionospheric and Saastamoinen tropospheric models have been applied. Navigation and observation RINEX files for both rover (smartphone) and base station (SORR) have been selected as inputs to RTKPOST (that is a RTKLIB module for post processing of GNSS data).

- Topcon Tools ver. 8.2.3, a commercial GNSS software, developed by Topcon Corporation. The software allows the processing of data from different devices such as total stations, digital levels and GNSS receivers, and it is used in many technical-scientific applications (Dawidowicz et al., 2015; Pa'suya et al., 2017). Topcon Tools uses the Modified Hopfield Model for the tropospheric corrections (Goad 1974). The employed positioning mode has been "CODE DIFF" (Code-based differential), and the time range and the cut-off angle have been set to 1 s and 10 degrees, respectively.

In the **Table 1** an overview of the settings used in the two software to obtain the positioning solution.

Table 1.

RTKlib and Topcon configurations used for the reference's computation.

Settings	RTKlib	Topcon
Positioning mode	Dual-frequency code-based differential	
Iono model	Klobuchar	Iono-free combination
Tropo model	Saastamoinen	Modified Hopfield
Mask angle	10°	
GNSS system	GPS, Glonass, BeiDou	GPS, Glonass
Base station	SORR (Sorrento, Naples) of Leica Italpos	

The ground truth has been chosen, comparing the solutions obtained with RTKlib and Topcon Tools in terms of solution availability and stability of the positioning estimates on vertical component.

The reference altitude is considered because one of the aim of the work is to provide an accurate estimation of the vertical component of the position, using the proposed SPP algorithm.

In **Fig. 3** the behavior of the two post-processed altitude values during the data collection is shown; in detail, the altitude solution computed using Topcon software is plotted in magenta line, while the altitude behavior obtained using RTKlib is represented by black line.

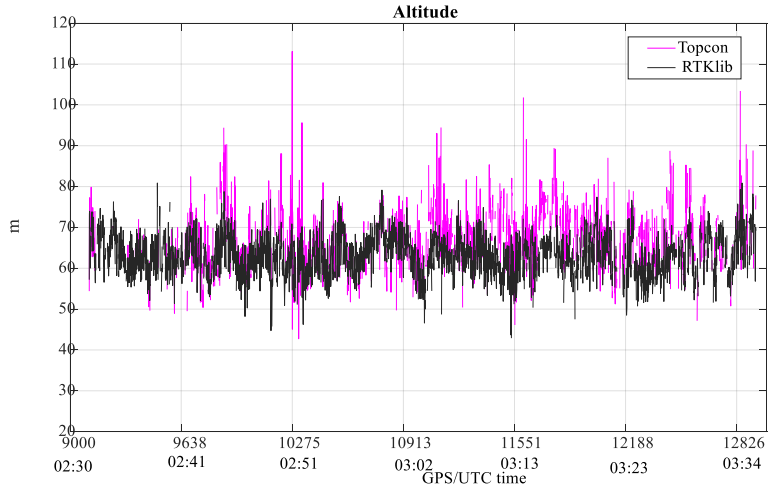

Fig. 3. comparison between altitude references obtained using RTKlib (black line) and Topcon (magenta line) software

From the figure, it can be highlighted that the altitude solution computed using RTKlib is more stable than Topcon solution. Indeed, for the altitude obtained with Topcon software, the mean value is 66.9 meters, the maximum is 113.1 meters and a standard deviation is 7.2 meters, while for the solution computed using RTKlib mean value, maximum value and standard deviation are respectively equal to 63.0, 80.9 and 5.0 meters. The altitude obtained with RTKlib has smaller peaks and less dispersion around the mean, hence it has a behavior more consistent with a ship motion.

The solution availability is the percentage of the epochs in which the software is able to provide positioning solution. Using RTKlib the solution availability is equal to 86.12 % while a lower solution availability is obtained using Topcon (52.8 %). The lower Topcon solution availability is related to the low quality of smartphone data, requiring more flexibility in the processing engine. Being Topcon Tools a professional software mainly for surveying and geodesy fields, it is designed for high quality data and based on very robust processing assumptions to deliver the most reliable solutions.

Based on these considerations, the RTKlib solution has been chosen as reference trajectory for the error analysis, with the purpose of verifying the performance of the proposed algorithm.

4. RESULTS

This section shows the experimental results obtained using the proposed SPP algorithm to process data collected during the kinematic test described in 3.1.

To verify both the benefit of GNSSs integration and the enhancement of the proposed algorithm especially on the estimation of the vertical component of position, different GNSS configurations are considered:

- GPS SPP-EKF (obtained processing only PR observables from GPS system);
- GLO (Glonass) SPP-EKF;
- BDS (BeiDou) SPP-EKF;
- GPS/GLO SPP-EKF (obtained processing only PR observables from GPS and Glonass systems);
- GPS/BDS SPP-EKF;
- BDS/GLO SPP-EKF;
- GPS/GLO/BDS SPP-EKF.

Furthermore, the SPP with WLS method is considered for comparison, using the same GNSSs combinations used for SPP-EKF approach.

After the data processing, the error analysis is carried out in position domain comparing the estimated solution with the RTKlib reference. The performance is evaluated in terms of RMS, mean and maximum error for both horizontal and vertical positioning errors.

Firstly, the improvements obtained using different GNSSs combinations in terms of satellite availability and geometry are analysed considering the number of available GNSS satellites and the satellite geometry, represented by the Position Dilution of Precision (PDOP). In **Table 2**, the minimum, maximum and mean values of PDOP and of number of visible satellites, for all the considered GNSS configurations, are shown. In addition, the solution availability is shown in the **Table 2**.

From the **Table 2**, it can be noted the improvement obtained thanks to the integration of GPS, Glonass and BeiDou satellites in terms of satellite visibility and geometry with the highest number of GNSS satellites and lowest values of PDOP. GPS-only, GPS/GLO and GPS/BDS configurations also show a good satellite geometry and high solution availability. Conversely, high PDOP values are obtained using only Glonass satellites with a maximum value of almost 30. The BDS satellites, visible diring the session, are 2 IGSO (Inclined geosynchronous orbits) and 6 MEO (Medium Earth orbits) and belongs to BDS-2 and BDS-3. BeiDou-only geometry seems better than Glonass one but is significantly worse with respect to GPS case.

The Glonass/BeiDou integration improves the satellite geometry. The best geometry is obtained, as expected, with the GPS/GLO/BDS configuration, which has PDOP values slightly lower than GPS-only case. Similarly, the solution availability of configurations including GPS is almost 100%, while the configurations without GPS are more discontinuous.

Table 2.

Statistical indicators of satellite visibility (as total number of visible satellites), geometry (as Position Dilution of Precision) and solution availability.

GNSS configuration	PDOP			Total number of SV			Solution Availability (%)
	Min	Max	Mean	Min	Max	Mean	
GPS	1.4	1.9	1.6	1	10	9.3	99.8
GLO	2.0	29.9	4.3	2	8	6.2	87.5
BDS	2.6	10.1	3.4	3	8	6.3	42.8
GPS/GLO	1.2	1.9	1.3	7	17	15.4	99.8
GPS/BDS	1.1	1.8	1.3	7	18	15.5	99.8
GLO/BDS	1.5	10.1	2.0	3	16	12.4	98.5
GPS/GLO/BDS	1.0	1.8	1.1	7	25	21.6	99.8

In **Fig. 4**, the number of GNSS satellites and PDOP behaviour are plotted as function of time only for GPS (green line), GLO (orange line), BDS (black line) and GPS/GLO/BDS (blue line) configurations.

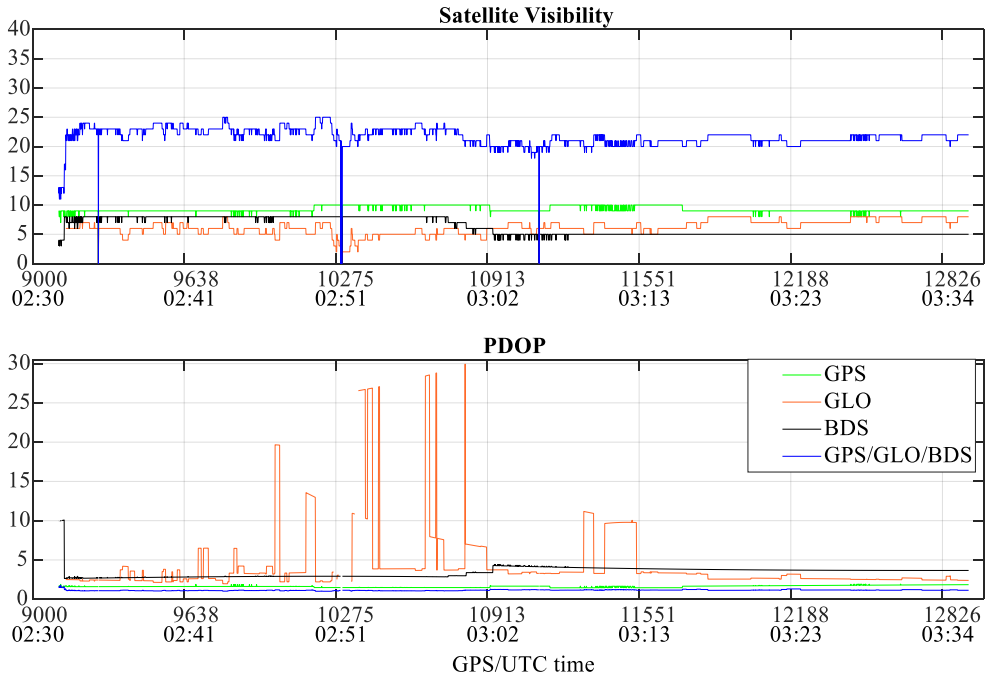

Fig. 4. Satellite visibility and PDOP behaviors for GPS (green line), GLO (orange line), BDS (black line) and GPS/GLO/BDS (blue line) configurations.

The figure confirms the results shown in **Table 2** and, in particular, the best performance of triple-GNSS constellation in terms of satellite visibility and geometry. Indeed, the number of satellites for GPS/GLO/BDS has a mean value of about 22 and PDOP mean value is equal to 1.1. However, all the

analysed GNSS configurations have shown three outages (with a duration of 1 second) due to a signal loss related to some failure of the receiver.

The **Table 3** summarizes the statistical parameters of the error analysis in the position domain for all the considered GNSS configurations and using two different estimators (EKF and WLS).

Table 1.

Summary Results for Horizontal (H) and Vertical (Up) component of the position obtained using the considered GNSS configurations and two different estimators (EKF and WLS).

PVT Algorithm	GNSS configuration	Mean Error		RMS		Max	
		H	Up	H	Up	H	Up
SPP EKF	GPS	3.39	0.03	4.00	3.87	19.27	15.82
	GLO	9.84	11.29	11.58	19.99	49.28	113.10
	BDS	8.27	4.73	9.64	18.24	32.90	72.08
	GPS/GLO	5.92	2.17	6.83	4.87	42.53	31.36
	GPS/BDS	5.87	0.81	7.51	5.52	33.66	29.00
	BDS/GLO	9.79	4.99	11.53	13.87	43.36	67.13
	GPS/GLO/BDS	6.51	0.18	7.76	5.57	31.52	27.50
SPP WLS	GPS	3.86	5.26	4.64	6.65	22.15	21.77
	GLO	11.77	12.48	14.17	28.11	88.67	269.24
	BDS	8.91	2.17	10.41	19.18	46.25	90.42
	GPS/GLO	5.77	2.49	6.73	4.97	42.55	31.16
	GPS/BDS	6.01	0.13	7.65	5.55	33.90	28.39
	BDS/GLO	9.95	4.30	11.80	14.88	57.44	93.81
	GPS/GLO/BDS	6.39	1.99	7.68	5.79	32.15	30.47

Comparing the configurations adopting different estimation techniques (EKF versus WLS), it can be noted that SPP-EKF provides significant improvement with respect to the WLS for all the analyzed figures of merit, especially on vertical component. In detail, an enhancement of meter order can be highlighted if GLO SPP-EKF is compared to GLO SPP-WLS on both vertical and horizontal component of the position. For all the other GNSS SPP-EKF configurations vertical mean error and RMS decrease by several meters compared with the corresponding GNSS SPP-WLS setting, while only an enhancement of decimeter level is evident for horizontal component of the position. The vertical errors for SPP-EKF configurations are lower than SPP-WLS due to the different adopted estimators and to the chosen setting of EKF. Indeed, EKF takes into account also the dynamic model in addition to measurements information, and the behaviour of the altitude of a ship during navigation has been taken into account choosing low variance values for the element of process noise matrix corresponding to vertical component. The same concept cannot be applied to latitude and longitude, so in EKF horizontal errors are larger than vertical ones.

About the benefit of GNSSs integration in the proposed algorithm, it can be noted that GPS-only configuration has the best performance in terms of all considered figures of merit. Conversely, GLO SPP-EKF has the worst behaviour with the highest statistical parameters' values, while a better accuracy solution is obtained using BDS SPP-EKF approach. Furthermore, the integration of Glonass satellites affects the accuracy of triple-GNSS constellation solution, that decreases with respect to GPS-only case. Considering dual-constellations, it can be noted that GPS/BDS SPP-EKF approach has better performance compared to GPS/GLO case, especially on vertical components with an enhancement of meter level. Finally, GPS/BDS SPP-EKF has statistical parameters values similar to GPS/GLO/BDS case. These results are related to the lower performance of Glonass and BeiDou systems compared to GPS in an open sky scenario.

About the expected worse performance of multi-GNSS configurations compared to GPS-only, in other work (Innac et al., 2018) the authors showed that, using multi-constellation, the enhancement in terms of accuracy is subject to the operational scenario and it is more evident in difficult environments for satellite navigation such as urban areas. However, benefits of the multi-constellation system in terms of integrity, availability and continuity are possible for any scenario, including an

open-sky scenario as confirmed by the solution availability, satellite visibility and geometry summarized in **Table 2**.

The same trend can be also highlighted for the configurations adopting WLS and comparing the several GNSS combinations: in fact, also in this case, GPS-only SPP-WLS has the best performance, especially on horizontal component. However, integrating GPS system with BeiDou or Glonass satellites, an accuracy improvement can be verified on vertical component of the position, especially for GPS/BDS integration, showing lower values of vertical mean error and RMS respect to single constellation setup. Also for SPP-WLS approach, the Glonass only configuration has the worst performance for all the figures of merit. Furthermore, considering GPS/GLO/BDS combination no evident enhancements in terms of accuracy can be seen due to the influence of Glonass measurements.

The values of horizontal and vertical RMS and mean errors for all the analysed GNSS configurations using the two SPP approaches are resumed in the **Fig. 5**. In the upper part of the plot, the statistical analysis for GNSS SPP-EKF is illustrated (where the blue bar indicating vertical mean error for GPS-only is not visible because is very low) while GNSS SPP –WLS performance are shown in the bottom.

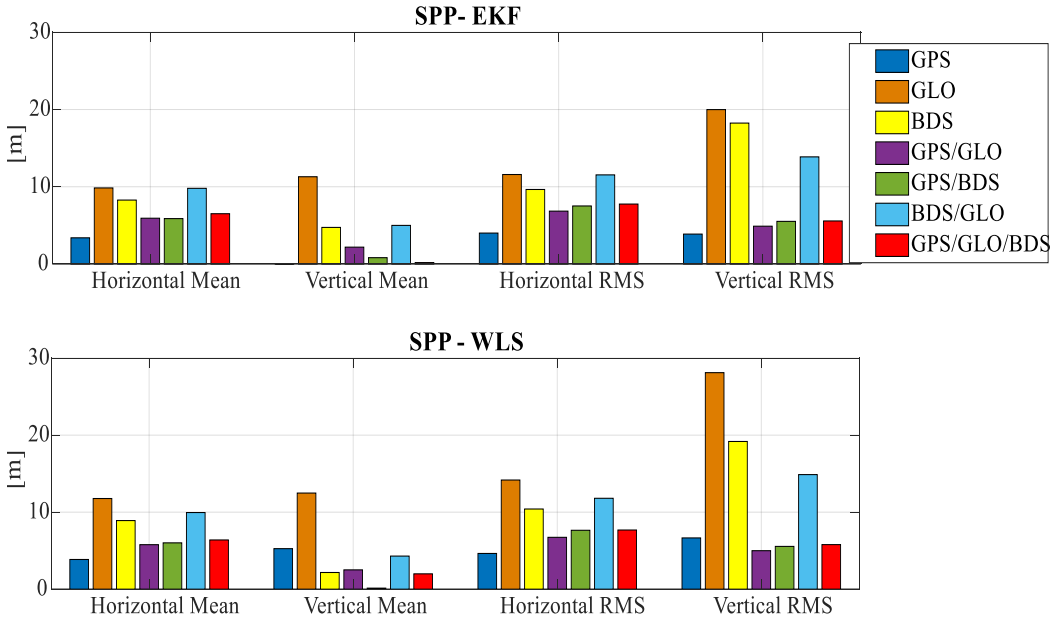

Fig. 5. RMS and Mean position errors for GPS (blue bar), Glonass (orange), BeiDou (yellow), GPS/GLO (violet), GPS/BDS (green), BDS/GLO (light blue) and GPS/GLO/BDS (red) using SPP-EKF and SPP- WLS approaches

A qualitative analysis is carried out comparing the two best solutions, obtained using the proposed SPP-EKF algorithm (GPS-only and GPS/GLO/BSD). Horizontal and vertical position errors, computed with respect to the reference solution, are plotted as a function of time in **Fig. 6** in which the green line is used for GPS SPP EKF and blue line for GPS/GLO/BDS SPP-EKF.

The figure confirms the experimental results previously described. The best configuration is GPS SPP-EKF showing the lowest positioning errors on both vertical and horizontal components. Conversely, GPS/GLO/BDS SPP-EKF solution accuracy slightly decreases in the epochs characterized by a higher satellite visibility due to the integration of BDS and GLO observables. These results are in line by literature (Angrisano et al., 2013; Innac et al., 2018) confirming that using the multi-constellation system in an open sky scenario, an enhancement in terms of availability and integrity is guaranteed but a position accuracy degradation of decimetre level could be obtained.

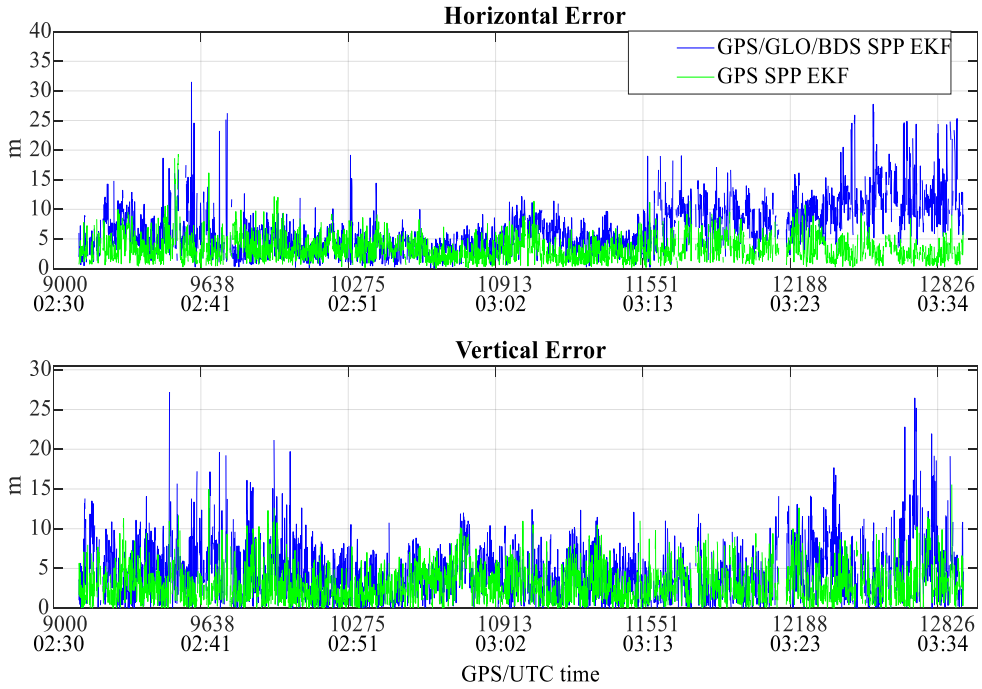

Fig. 6. Horizontal and vertical positioning errors for the considered configurations: for GPS SPP EKF (green line) and for GPS/GLO/BDS SPP-EKF (blue line)

5. CONCLUSIONS

The precise positioning techniques (RTK or PPP), commonly used for maritime applications, are limited by different factors such as the application of corrections transmitted by stations located nearby, long convergence times due to the ambiguity resolution problem and the use of high-quality GNSS receivers and antennas. The main objective of the work is to provide a positioning technique, usable in maritime applications and based on low cost equipment.

The vertical component of the position is a key parameter for the analysis of the sea conditions, which starts from the survey of the amplitudes of the vessel motions. Therefore, for related applications, it is fundamental to estimate accurately the altitude.

A low cost positioning, which estimates accurately the altitude, is suitable for small boats (to support the navigation) or passenger of large ships (to provide information about the sea conditions).

A GNSS receiver embedded in a smartphone has been chosen for the experiment in this work.

The proposed algorithm allows global coverage for offshore applications, extending the ability to obtain acceptable accuracy even in remote areas, reducing the costs and logistic requirements necessary for maritime applications.

A SPP algorithm has been implemented using a EKF approach finely tuned to improve the altitude estimates. The proposed algorithm has been tested using a kinematic data collection performed locating a smartphone on board a ferryboat travelling Mediterranean Sea. GPS, Glonass and BeiDou PR observables have been processed using the proposed algorithm and its performance are evaluated in position domain and compared to SPP-WLS approach (that is SPP with Weighted Least Square estimator). Carrier phase measurements are not included in the processing, because of their inherent instability, typical of smartphone GNSS chips. Furthermore, different GNSSs combinations have been considered and their contribution in terms of accuracy, solution availability, satellite visibility and geometry has been analysed.

Experimental results have highlighted that SPP-EKF provides an enhancement of meter order on vertical component of the position, while a slightly improvement is evident on horizontal plane as expected from the setting of the covariance matrix of the process noise. Considering the obtained performance, based on the analysed data, the algorithm can be used for applications that need to determine the sea conditions that can cause a state of discomfort for the user on board the ship and for small boats. However, the performance of the proposed algorithm, using data collected by high grade receivers, will be analysed in future works.

About the benefit of the GNSSs integration, the results have shown that GPS-only configuration has better performance with respect to other GNSSs configurations in terms of accuracy, while an enhancement in terms of satellite availability and geometry is obtained thanks to the integration of GPS, Glonass and BeiDou observables. However, as well known, the benefit of multi-GNSS constellation in terms of accuracy could be exploited in an urban environment where the presence of obstacles creates a complex operational scenario, characterized by blocking and multipath phenomena.

ACKNOWLEDGMENTS

The work was supported by “DORA - Deployable Optics for Remote sensing Applications DORA” (ARS01_00653), a project funded by MIUR - PON “Research & Innovation”/PNR 2015-2020.

REFERENCES

Alkan, R. M. and Öcalan, T. (2013). Usability of the GPS precise point positioning technique in marine applications. The Journal of Navigation, 66(4), 579–588.

Angrisano, A., Gaglione, S., Gioia, C. (2013) Performance assessment of GPS/GLONASS single point positioning in an urban environment. Acta Geodaetica et Geophysica, 48(2), 149-161.

Constantin-Octavian, A. (2012) Cost-effective precise positioning using carrier phase navigation-grade receiver. In 2012 International Conference on Localization and GNSS, 1-6. IEEE.

Dawidowicz, K., Krzan, G., Świątek, K. (2015) Relative GPS/GLONASS coordinates determination in urban areas-accuracy analysis. In Proceedings of 15th edition of SGEM GeoConferences, 2, 423-430, Bulgaria, 2015.

El-Mowafy, A. (2012) Precise real-time positioning using Network RTK. Global navigation satellite systems: signal, theory and applications, 161-189.

Goad, C. C. (1974) A modified Hopfield tropospheric refraction correction model. In Proceedings of the Fall Annual Meeting American Geophysical Union.

Hoffmann-Wellenhof, B., Lichtenegger, H., Collins, J. (1992) Global Positioning System: Theory and Practice. Springer.

Innac, A., Gaglione, S., Angrisano, A. (2018) Multi-GNSS Single Frequency Precise Point Positioning. In Proceedings of IEEE International Workshop on Metrology for the Sea, Learning to Measure Sea Health Parameters (MetroSea 2018), 222-226. IEEE.

IOC - International Oceanographic Commission, (2006) Manual on seal level measurement and interpretation, vol. IV, JCOMM technical report No 31, UNESCO.

Kalman, R.E. (1960) A new approach to linear filtering and prediction problems. Trans ASME J Basic Eng, 35–45.

Kaplan, E.D., Hegarty, (2006) C. Understanding GPS: Principles and Applications, Artech House Mobile Communications Series.

Lachapelle, G., Gratton, P., Horrelt, J., Lemieux, E., & Broumandan, A. (2018) Evaluation of a low cost hand held unit with GNSS raw data capability and comparison with an android smartphone. Sensors, 18(12), 4185.

Li, X., Ge, M., Dai, X., Ren, X., Fritsche, M., Wickert, J., & Schuh, H. (2015) Accuracy and reliability of multi-GNSS real-time precise positioning: GPS, GLONASS, BeiDou, and Galileo. Journal of Geodesy, 89(6), 607-635.

Marreiros, J.P.R. (2013) Kinematic GNSS Precise Point Positioning: Application to Marine Platforms. Ph.D. Thesis, University of Porto, Porto, Portugal.

Montazeri, N., Nielsen, U.D., Jensen, J.J. (2016) Estimation of wind sea and swell using shipboard measurements – A refined parametric modelling approach. Applied Ocean Research, 54, 73-86.

Parkinson, B. W., Enge, P., Axelrad, P., Spilker Jr, J. J. (1996) Global positioning system: Theory and applications, Volume II. American Institute of Aeronautics and Astronautics.

Pa'suya, M. F., Din, A. H. M., Amin, Z. M., Omar, K. M., Omar, A. H., & Rusli, N. (2017) Evaluation of Global Digital Elevation Model for Flood Risk Management in Perlis. In Proceedings of Global Civil Engineering Conference, 1007-1017.

Paziewski, J., Wielgosz, P. (2017) Investigation of some selected strategies for multi-GNSS instantaneous RTK positioning. Advances in Space Research, 59(1), 12-23.

Paziewski, J., Sieradzki, R., Baryla, R. (2019) Signal Characterization and Assessment of Code GNSS Positioning with Low-Power Consumption Smartphones. GPS Solution, 23, 98

Paziewski, J. (2020) Recent advances and perspectives for positioning and applications with smartphone GNSS observations. Meas. Sci. Technol, 31(091001).

Piscopo, V., Scamardella, A., & Gaglione, S. (2020). A new wave spectrum resembling procedure based on ship motion analysis. Ocean Engineering, 201, 107137.

Realini, E., Caldera, S., Pertusini, L., Sampietro, D. (2017) Precise GNSS positioning using smart devices. Sensors, Vol. 17(10), 2434.

Reinking, J., Härting, A., Bastos, L. (2012) Determination of sea surface height from moving ships with dynamic corrections. Journal of Geodetic Science, 2(3), 172-187.

Robustelli, U., Baiocchi, V., Pugliano, G. (2019) Assessment of dual frequency GNSS observations from a Xiaomi Mi 8 Android smartphone and positioning performance analysis. Electronics, 8(1), 91.

Specht, C., Pawelski, J., Smolarek, L., Specht, M., Dabrowski, P. (2019) Assessment of the positioning accuracy of DGPS and EGNOS systems in the Bay of Gdansk using maritime dynamic measurements. The Journal of Navigation, 72(3), 575-587.

Specht, C., Dabrowski, P. S., Pawelski, J., Specht, M., Szot, T. (2019) Comparative analysis of positioning accuracy of GNSS receivers of Samsung Galaxy smartphones in marine dynamic measurements. Advances in Space Research, 63(9), 3018-3028.

Sørensen, A. J. (2011) A survey of dynamic positioning control systems. Annual reviews in control, 35(1), 123-136.

Takasu, T., Kubo, N., Yasuda, A. (2007) Development, evaluation and application of RTKLIB: a program library for RTK-GPS. In Proceedings of GPS/GNSS symposium, 213-218.

Teunissen, P. J., Giorgi, G., Buist, P. J. (2011) Testing of a new single-frequency GNSS carrier phase attitude determination method: land, ship and aircraft experiments. GPS solutions, Vol. 15(1), 15-28.

Welch, G., Bishop, G. (2004) An Introduction to the Kalman Filter, University of North Carolina at Chapter Hill, Chapter Hill. TR 95-014, April 5, 2004.